Acta Cryst. (1982). A**38**, 648–656

Experimental Correction for Primary and Secondary Extinction. II. Application to Beryllium

BY P. SUORTTI

Department of Physics, University of Helsinki, Siltavuorenpenger 20 D, 00170 Helsinki 17, Finland

(*Received* 11 *August* 1981; *accepted* 19 *April* 1982)

Abstract

The profiles of the first three reflections from a parallel-sided crystal slab of Be are measured on an absolute scale with polarized Cu $K\alpha$ radiation and unpolarized Mo $K\alpha$ radiation. The effects of secondary extinction are corrected by measuring the transmitted intensity and using the conservation of energy. Primary extinction is determined by comparing two measurements where the extinction distances are different; this is realized by changing the wavelength or polarization of the incident radiation. The calculated average secondary-extinction factor, $\overline{y_s}$, ranges from 0·98 to 0·74, and the average primary extinction factor, $\overline{y_p}$, from 0·96 to 0·42. The room-temperature values of the structure factors, $F(10.1) = 1{\cdot}90 \pm 0{\cdot}01$, $F(00.2) = 3{\cdot}37 \pm 0{\cdot}02$, $F(10.1) = 2{\cdot}78 \pm 0{\cdot}03$, differ substantially from earlier experimental values and from the values calculated for a free atom, but agree very closely with the results of a LCAO calculation.

1. Introduction

In the preceding paper (Suortti, 1982; hereafter I) a phenomenological separation of primary and secondary extinction was made. This separation has an operational meaning as the coupling constant of the incoherent intensity fields, *i.e.* the correction for secondary extinction, is proportional to the measured reflectivity, and on the other hand the coupling between coherent fields can be varied by changing the parameters that determine the extinction distance. This paper describes a realization of these ideas, and the experimental conditions are discussed at length.

The sample crystal in the present measurement is Be. It has small absorption for crystallographic X-ray wavelengths, and therefore Laue diffraction from fairly thick crystal slabs is feasible. The first three reflections 10.0, 00.2 and 10.1 can be measured in the symmetrical arrangement from the same crystal. These reflections carry information of the bonding effects of solid Be, which have been subjects of great interest in the last few years. The early measurement by Brown (1972), its analysis (Stewart, 1977; Yang & Coppens, 1978) and some theoretical work (Inoue & Yamashita, 1973; Matthai, Grout & March, 1980) suggest significant p character of the bonding and general expansion of the atom. Recent measurements, however, show that a free-atom calculation gives an adequate description of the 1s core (Manninen & Suortti, 1979; Larsen, Lehmann & Merisalo, 1980) and that the bonding effects are far less dramatic than those suggested by the early work (Larsen, Hansen & Schneider, 1981).

Compton profile measurements and related theoretical work on Be has been recently summarized by Loupias, Petiau, Issolah & Schneider (1980). The best overall picture is given by LCAO calculations, although there are still some discrepancies between theory and experiment. The observed differences between directional Compton profiles are large enough to correspond to substantial effects of anisotropy also in the scattering factors. New independent data are needed, and this makes Be an interesting subject of study, while at the same time Be is a suitable test case for the present method.

2. Reflectivity and primary extinction

The reflecting ratio $r(\varepsilon)$ can be determined directly from the reduction of the direct beam in the symmetrical Laue geometry, equation (I,16a,b),

$$\frac{1}{1 + r(\varepsilon)} \simeq 1 - \frac{P_g^*(\varepsilon)}{P_0 \exp(-\mu_0 T/\cos\theta)}, \qquad (1)$$

where $P_g^*(\varepsilon)$ is the observed diffracted power and $P_0 \exp(-\mu_0 T/\cos\theta)$ is the transmitted direct beam when there is no diffraction. T is the thickness of the crystal and μ_0 the linear attenuation coefficient, which arises from photoelectric absorption and inelastic scattering. The observed reflecting ratio is

$$r^*(\varepsilon) \simeq r(\varepsilon)/\{1 + r(\varepsilon) + \tfrac{1}{3}[r(\varepsilon)]^2\}, \qquad (2)$$

and so $r(\varepsilon)$ is the reflecting ratio as corrected for secondary extinction. The corresponding integrated intensity is

$$E = \frac{1}{\omega} \exp(-\mu_0 T/\cos\theta) \int r(\varepsilon)\, d\varepsilon, \qquad (I,20a)$$

where ω is the angular velocity of the crystal.

0567-7394/82/050648-09$01.00

The degree of primary extinction depends on the effective size of the coherent domain, and this can be varied by varying the extinction distance Λ. Consider two measurements, indicated by subscripts 1 and 2. From (I,13) and (I,14),

$$y_{p,i}(\varepsilon)\, w_i(\varepsilon) = Q_i^{-1}\, \overline{\sigma_i(\varepsilon)} \simeq \exp\{-(\alpha_i' \delta_i)^2\}\, w_i(\varepsilon), \quad i = 1, 2, \tag{3}$$

where $\delta_i = \overline{\delta_i(\varepsilon)} = \overline{D(\varepsilon)}/\Lambda_i$. If the crystal volume illuminated by the incident beam is the same in both cases, $w_1(\varepsilon) = w_2(\varepsilon)$ and $\alpha_1' = \alpha_2' = \alpha'$, and

$$f(\varepsilon) = \frac{y_{p,1}(\varepsilon)}{y_{p,2}(\varepsilon)} = \exp\{-(\alpha'\, \delta_1)^2[1 - (\delta_2/\delta_1)^2]\} = \frac{Q_2}{Q_1}\frac{\overline{\sigma_1}(\varepsilon)}{\overline{\sigma_2}(\varepsilon)}. \tag{4a}$$

The correction for primary extinction is

$$y_{p,1}(\varepsilon) = \{f(\varepsilon)\}^{\beta}, \tag{4b}$$

where

$$\beta^{-1} = 1 - (\Lambda_1/\Lambda_2)^2. \tag{4c}$$

The extinction distance is given by

$$\Lambda = V_c/(\lambda C r_e F_g H), \tag{4d}$$

where V_c is the volume of the unit cell with structure factor F_g, λ is the X-ray wavelength, C the polarization factor, r_e the electron scattering length, and H the long-range-order parameter, which for a perfect crystal is the Debye–Waller factor $\exp(-M)$. The correction for primary extinction can be calculated at each point of the reflection profile from the measured reflecting ratios $r_1(\varepsilon)$ and $r_2(\varepsilon)$.

The extinction distance Λ can be varied by changing the polarization factor C or the wavelength λ. A change in λ usually entails a change of C, and

$$\beta_\lambda^{-1} = 1 - (\lambda_2 C_2/\lambda_1 C_1)^2. \tag{5a}$$

If the polarization of the beam is parallel to the plane of diffraction in one measurement, $C_1 = \cos|2\theta|$, and perpendicular to this plane in the other, $C_2 = 1$,

$$\beta_C^{-1} = 1 - \sec^2 2\theta. \tag{5b}$$

The third possibility where major changes in F_g are introduced by varying λ near an absorption edge is feasible only when the anomalous scattering factors are known accurately.

Variation of Λ by changing the polarization factor C is the ideal method from the experimental point of view, because the other factors stay unchanged. The active volume of the sample crystal can be kept the same in the two measurements, as required for an accurate determination of $y_p(\varepsilon)$. However, there are a few practical difficulties. The wavelength must be long enough to make β_C^{-1} sufficiently different from zero even for the strong low-order reflections, because otherwise $f(\varepsilon) \simeq 1$, and the statistical fluctuations are enhanced. In this situation absorption may allow use of very thin samples only. The divergences of the incident beam should be about 0·1 mrad in both directions, which means an impractically low power of the beam, when a conventional X-ray source is used. This is the most serious limitation of the present experiment, and will be discussed in detail later on.

The X-ray wavelength is an effective way of varying Λ, but problems arise from the unavoidable changes of the illuminated crystal volume. If the Bragg angles are small and the incident beam wide in comparison with the thickness of the crystal, the changes in the active volume may not be serious. It was noted before that $y_p(\varepsilon)$ can be defined only as an average taken over $\Delta\varepsilon \simeq 10\lambda|\kappa_g|$, which must be covered by beam divergences and/or continuous scan. Another practical problem is the comparison of absolute intensities measured with different radiations.

The integrated intensity which is corrected for secondary and primary extinctions is

$$E_{\text{kin}} = \frac{1}{\omega}\exp(-\mu_0 T/\cos\theta)\int \{f(\varepsilon)\}^{-\beta} r_1(\varepsilon)\, \mathrm{d}\varepsilon. \tag{6a}$$

In the case of symmetrical Laue diffraction from a crystal slab of thickness T,

$$E_{\text{kin}} = \frac{1}{\omega}\exp(-\mu_0 T/\cos\theta)\frac{r_e^2\lambda^3}{V_c^2}F_g^2\frac{K_{\text{pol}}}{\sin 2\theta}\frac{T}{\cos\theta}, \tag{6b}$$

where K_{pol} is the polarization factor appropriate for the kinematical case.

3. Experimental conditions

The ideal measuring conditions for the application of the present method are such that the incident beam is strictly parallel and the scan over the reflection is made in small pieces $\Delta\varepsilon$, each one large enough to yield a well-defined primary extinction factor $y_p(\varepsilon)$. In practice, $\Delta\varepsilon$ is covered by a combination of beam divergences and scan, but (I,15) and (I,16) are valid only when this angular range is small in comparison with the width of the reflection. Otherwise, the measured profile must be first deconvoluted by the instrument function; this has been considered in the case where the true reflection and instrument function profiles can be approximated by Gaussians (DeMarco, Diana & Mazzone, 1967). The wavelength spread of the incident beam is equally important. The monochromated characteristic radiation from an X-ray tube contains both α_1 and α_2 components, and the corresponding Bragg angles of the sample crystal usually differ by more than the permissible $\Delta\varepsilon$. This situation has been overlooked in the earlier applications of the method, and the corrections for secondary extinction have been under-

estimated by an amount that corresponds to smearing of the reflecting ratio $r(\varepsilon)$.

The reflection widths of the Be single crystal varied from 1 to 10 mrad, and suitable divergences of the incident beam were obtained by a reflection from a perfect crystal. The 220 reflections of Si and Ge were used; for Ge 220 the Darwin width is about 0·1 mrad for Cu $K\alpha$ and 0·04 mrad for Mo $K\alpha$, and the corresponding values for Si 220 are about $\frac{1}{3}$ of these widths. The broadening due to the wavelength dispersion can be reduced to the same level by a (+,−) arrangement of the monochromator and the sample crystal, because the Bragg angles of Be 10.0, Be 00.2 and Be 10.1 are quite close to those of the 220 reflection of Si or Ge. The maximum effect of wavelength dispersion in the non-dispersive arrangements of Fig. 1 were $\Delta\theta = 0{\cdot}2$ mrad.

The present measurements were made with polarized Cu $K\alpha$ radiation and almost unpolarized Mo $K\alpha$ radiation. Anomalous transmission or Borrmann effect was utilized for production of a polarized X-ray beam. Radiation from the point focus of a Cu target tube passed through antiscatter slits, the polarizing crystal, and a circular aperture of about 1 mm diameter before hitting the sample crystal. The polarizer is essentially a goniometer where a perfect Ge crystal can be rotated about the surface normal and rocked with respect to the incident beam. The Ge crystal is cut parallel to the (111) planes, and Laue diffraction takes place from the (2$\bar{2}$0) planes (Cole, Chambers & Wood, 1961). The plane of polarization is changed by rotating the whole goniometer about the incident beam; this is realized by a telescope construction. The thickness of the Ge crystal is about 1 mm, and a sufficient flux of $P_0\exp(-\mu_0 T/\cos\theta) \simeq 5 \times 10^3$ c s^{-1} and spectral purity for an absolute measurement was obtained by the X-ray tube ratings 30 kV, 20 mA. The degree of linear polarization was measured with a 90° reflection polarizer (Suortti & Jennings, 1977), and it was found to be practically 100%. Mo $K\alpha$ radiation could also be polarized in this way, but the intensity remained impractically low, $P_0 \simeq 10^3$ c s^{-1}, and changing the polarization factor C has too small an effect on the extinction distance to facilitate a reliable determination of $y_p(\varepsilon)$.

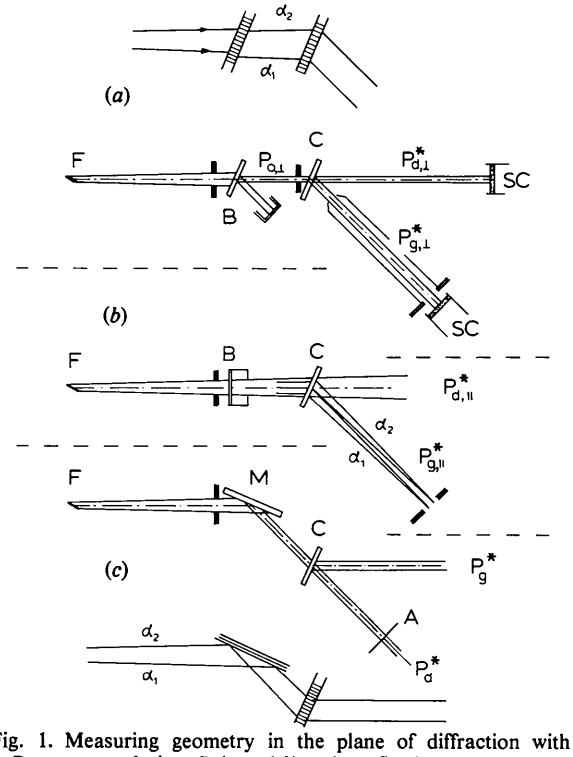

Fig. 1. Measuring geometry in the plane of diffraction with a Borrmann polarizer B (a and b) and a reflecting monochromator M (c). The point focus of the X-ray tube is indicated by F, the sample crystal by C, and the scintillation counter by SC. The forward diffracted beam from the polarizer is used, and the other beam is caught by a beam stop shown in (a). The inserts in (a) and (c) show the non-dispersive setting when the Bragg angle of the polarizer or monochromator is equal to that of the sample crystal.

Radiation from a Mo target tube was monochromated by the 220 reflection of Ge or Si. Point focus of the tube was used as above in order to produce a uniform distribution of intensity in the incident beam. The beam contains two components of polarization with relative weights 1 and $K = |\cos 2\theta_m|$, where θ_m is the Bragg angle of the monochromator. These components should be carried separately through (4a) to (4c), which makes the polarization factor in (5a) quite cumbersome. In the present case it was found sufficient to write $C = (1 + K|\cos 2\theta|)/(1 + K)$, which corresponds to using an average extinction distance in (4c).

The reflections were measured with a step-wise θ–2θ scan, which maintained the symmetrical transmission geometry. Most of the scattering from air and slit edges was eliminated by a diffracted beam tunnel. The 2 × 2° opening of the receiving slit was small enough to keep the TDS contribution to the low-order reflections of Be negligible (Kurittu & Merisalo, 1977; Merisalo & Kurittu, 1978), and only a linear subtraction of background was made. Uniform response of the scintillation counter was checked over the active area, and the same counter was used to measure also the direct beam. The incident flux of the polarized X-rays was small enough to be measured without attenuators, while the Mo $K\alpha$ beam from the reflection monochromator had to be attenuated by a Mo foil. The attenuation factor and the dead time of the counting chain was determined by the procedure described by Chipman (1968). The measurement of the reflections was automated by use of a programmable control unit with a tape reader/punch and teletype as the input/output device.

The sample crystal was spark cut from a bar of Be single crystal. The effective thickness of the crystal slab

was 1·118 ± 0·005 mm, and its normal coincided with the [12.0] direction within 2°; the observed intensities were corrected for the effects of miscut. Reflections of type $h0.l$ can be measured in the symmetrical Laue geometry. The crystal was distorted by pressing, and a slight non-parallelism of the pressing surfaces produced various degrees of faulting. This was observed by scanning the 10.0 and 00.2 reflections at about 30 points over the crystal face. Upon squeezing, the slight surface roughness was useful, because no macroscopic slipping was observable, while this was very clear in polished crystals. However, a very non-uniform mosaic structure was found, and the measurements were made only at locations where the rocking curves were reasonably smooth. Extensive measurements of the background intensity showed that there was no observable scattering from a possible polycrystalline surface layer. For the movements of the crystal a special goniometer was built, where the crystal could be rotated about the surface normal and translated perpendicular to the normal. The incident beam was accurately aligned to the center of the goniometer, so that the same place stayed illuminated when the crystal was rotated.

4. Measurements with two wavelengths

The geometries (*a*) and (*c*) shown in Fig. 1 are both sufficiently non-dispersive to make the correction for secondary extinction straightforward, and the reflecting ratios measured with Cu $K\alpha$ and Mo $K\alpha$ can be compared for a determination of the correction for primary extinction. In each case, the reflecting ratio $r(\varepsilon)$ is calculated from the measured diffracted photon flux and the flux of the transmitted direct beam using (1) and (2). The two profiles recorded at the same location in the crystal with Cu $K\alpha$ and Mo $K\alpha$ radiations are compared through the function $f(\varepsilon)$, and the correction for primary extinction can be calculated from (4) and (5*a*). The parameters used in the calculations are given in Table 1.

Table 1. *Experimental parameters in measurements with* Cu $K\alpha$ *and* Mo $K\alpha$ *radiations*

The kinematical integrated reflecting ratio is $A_{kin} = \int r_{kin}(\varepsilon)\,d\varepsilon = Q(T/\cos\theta)$. The polarization factor in Q is $K_{pol} = (1 + K\cos^2 2\theta)/(1 + K)$, where $K = P_{0,\parallel}/P_{0,\perp}$.

	$\lambda = 1{\cdot}5418$ Å, $K = 0$		$\lambda = 0{\cdot}7107$ Å, $K = 0{\cdot}9315$		
hk.l	2θ	A_{kin}/F_g^2	2θ	A_{kin}/F_g^2	β_λ
10.0	45·84	$1{\cdot}8721 \times 10^{-4}$	20·68	$0{\cdot}3277 \times 10^{-4}$	−0·2492
00.2	50·95	1·7636	22·87	0·2948	−0·2448
10.1	52·83	1·7326	23·67	0·2843	−0·2431

The above procedure does not work in all cases, because the profiles measured with different wavelengths could not always be matched. The illuminated volume increases with wavelength in the present geometry, and in many cases the profiles measured with Cu $K\alpha$ radiation were wider than the corresponding profiles measured with Mo $K\alpha$. However, there were a sufficient number of favorable cases for each reflection, and a few representative profiles are shown in Fig. 2, while the corresponding values of the structure factors are included in Table 2.

The correction for primary extinction, given by $y_p^{-1}(\varepsilon) - 1$, is shown in Fig. 2 as well. Much of the details towards the tails of the reflections are artefacts due to the differences in the distributions of the coherent domains, but nevertheless some conclusions

Table 2. *Integrated reflecting ratios A at various locations of the* Be *crystal measured with* Cu $K\alpha$ *and* Mo $K\alpha$ *radiations*

The approximate half-widths of the reflections are given by $\Delta\varepsilon$; D_m is the maximum size of the coherent domain as estimated from equation (7). The average amount of secondary and primary extinctions are given by $\overline{y_s}$ and $\overline{y_p}$, respectively. The structure factor F_g is calculated from the corrected reflecting ratio A_{kin}, and the corresponding dynamical value A_{dyn} is given for comparison.

hk.l	location	D_m (μm)	$\Delta\varepsilon$ (°)		$A_{meas} \times 10^3$	$\overline{y_s}$	$\overline{y_p}$	$A_{kin} \times 10^3$	$A_{dyn} \times 10^5$	F_g
10.0	(0·5, −1)	15	0·2	Cu $K\alpha$	0·4708	0·915	0·778	0·6617	0·541	1·88
				Mo $K\alpha$	0·1065	0·982	0·936	0·1158	0·226	
	(−2, 4)		0·03	Cu $K\alpha$	0·2390	0·831	0·426	0·6758	0·547	1·90
				Mo $K\alpha$	0·0877	0·907	0·820	0·1183	0·229	
00.2	(−1, 0)	30	0·2	Cu $K\alpha$	1·4245	0·831	0·867	1·9792	0·891	3·35
				Mo $K\alpha$	0·3058	0·964	0·959	0·3308	0·364	
	(−2, 4)		0·03	Cu $K\alpha$	0·5649	0·798	0·424	1·6730	0·819	3·08
				Mo $K\alpha$	0·1990	0·876	0·812	0·2797	0·335	
10.1	(−1, 0)	20	0·2	Cu $K\alpha$	0·9198	0·852	0·801	1·3487	0·723	2·79
				Mo $K\alpha$	0·2006	0·963	0·941	0·2213	0·293	
	(−2, 4)		0·04	Cu $K\alpha$	0·4936	0·740	0·467	1·4271	0·743	2·87
				Mo $K\alpha$	0·1737	0·883	0·840	0·2342	0·301	

on the relationship between $r(\varepsilon)$ and $y_p^{-1} - 1$ can be made.

In the cases of narrow reflections, where the corrections for both secondary and primary extinctions are large, $y_p^{-1}(\varepsilon) - 1$ resembles the reflection profile. Equation (3) gives in the first approximation that

$$y_p^{-1}(\varepsilon) - 1 \simeq \{\alpha' \, \delta(\varepsilon)\}^2, \qquad (7)$$

and so the peaks of the reflections correspond to the largest coherent domains. The size of the domains, D can be estimated from (7) by taking $\alpha' = 0{\cdot}5$ (Olekhnovich, Markovich & Olekhnovich, 1980), and a few values are given in Table 2.

The wide reflections show mixed behavior. In some cases, such as 10.1 measured at location (−1,0), the correction for primary extinction is practically constant. In this case the size distribution of the coherent domains is not correlated with the orientation distribution, which determines the reflection profile. The profile of 00.2 at (−1,0) suggests that the crystal is broken into several major blocks, which differ in orientation by angles of the order of 0·1°, and the effect of two crystal blocks is clearly seen in 10.1 measured at (−2,4). The shape of 10.0 at (0·5,−1) is due to an asymmetric distribution of larger domains.

Another comparison of the reflectivity curves is shown in Fig. 3. The normalized ratio from (4*a*) is

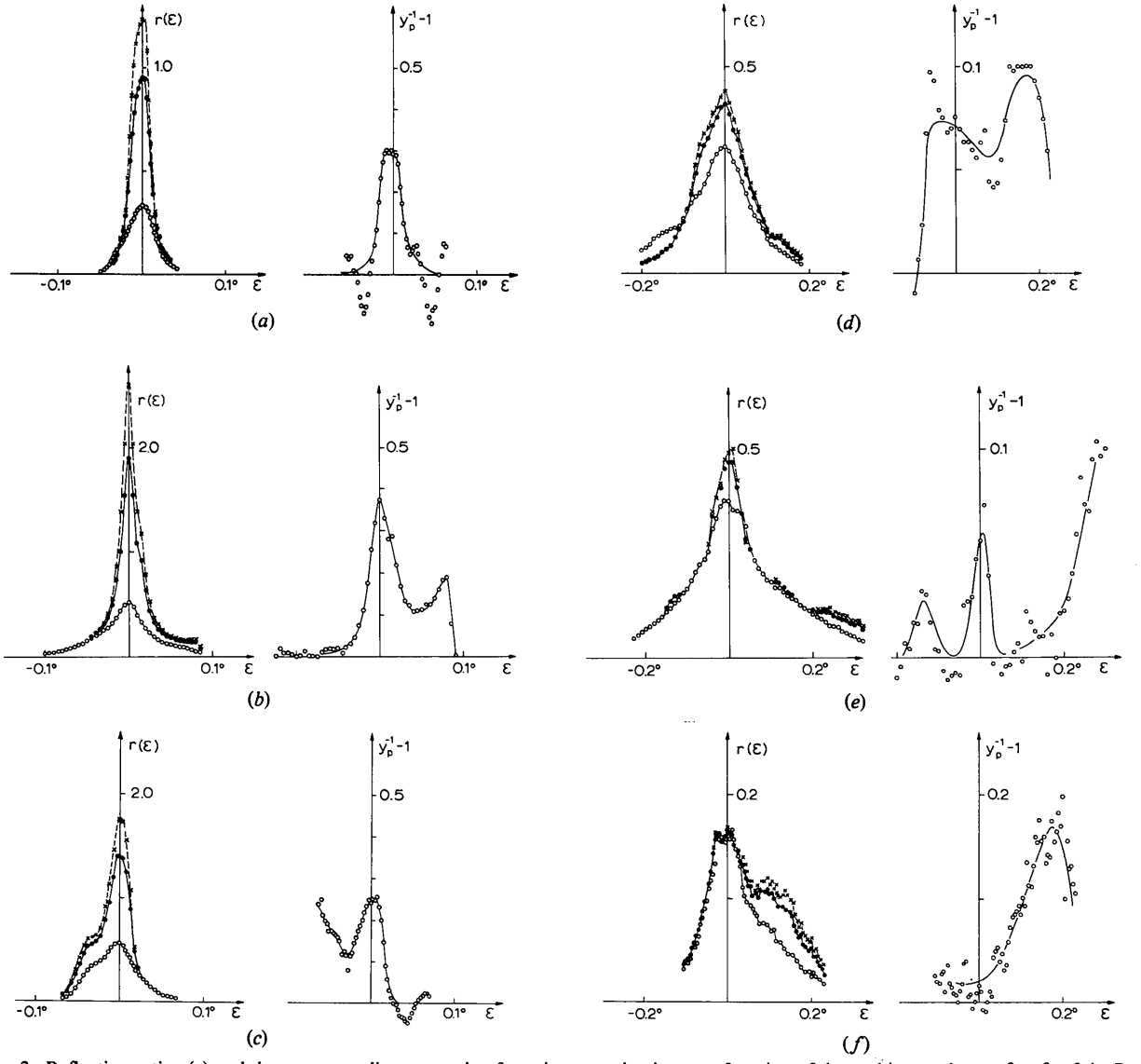

Fig. 2. Reflecting ratio $r(\varepsilon)$ and the corresponding correction for primary extinction as a function of the rocking angle $\varepsilon = \theta - \theta_B$ of the Be crystal. Open circles (○) give $r(\varepsilon) = r_2(\varepsilon)$ with Cu $K\alpha$ radiation and the results with Mo $K\alpha$ are brought to the same scale by multiplying by $(Q_2/Q_1)(\cos\theta_1/\cos\theta_2)$; filled circles (●) indicate $r(\varepsilon) = r_1(\varepsilon)$ before and crosses (×) after the correction for primary extinction. (*a*) 10.0 at (−2,4); (*b*) 00.2 at (−2,4); (*c*) 10.1 at (−2,4); (*d*) 10.1 at (−1,0); (*e*) 00.2 at (−1,0); (*f*) 10.0 at (0·5, −1).

given before and after the correction for secondary extinction by $f^*(\varepsilon)$ and $f(\varepsilon)$, respectively. The curves are similar to those given by $y_p^{-1}(\varepsilon) - 1$, but the features are more pronounced, as in (4*b*) $\beta \simeq -0{\cdot}25$ in the present case. The findings are similar to those of Olekhnovich, Markovich & Olekhnovich (1980): for a wide reflection $f^*(\varepsilon) - 1$ or $f(\varepsilon) - 1$ is quite constant within the range of reflection and zero outside, while in the case of a narrow reflection these curves resemble the reflection profile. Olekhnovich *et al.* (1980) interpreted the results within the mosaic-crystal model, partly utilizing the specific results of Zachariasen (1967), and primary extinction was considered predominant in the case of wide reflections [or constant $f^*(\varepsilon) - 1$], while the narrow reflections were taken to exhibit mostly secondary extinction. The present result is quite different. The values of the average extinction corrections for a few reflections are given in Table 2, and these demonstrate that primary and secondary extinctions always coexist. For a wide reflection the corrections are of the same magnitude, but primary extinction becomes dominant in the narrow reflections. This is particularly clear in the results obtained by Cu $K\alpha$ radiation, when the extinction distance is decreased by a factor of 2·2 from that for Mo $K\alpha$ radiation.

The difference between the interpretation by Olekhnovich *et al.* (1980) and the present conclusions arises from the limitations of the mosaic-crystal model: there is no correlation between the orientation and size distributions of the mosaics. This implies a constant primary extinction over the profile, and secondary extinction may be classified as orientation-determined (type I) or size-determined (type II), according to Zachariasen (1967). The present results indicate, however, that particularly in the case of a narrow regularly shaped reflection the size of the coherent domains is maximum at $\varepsilon = 0$. Primary and secondary extinctions both follow the shape of the reflection profile, and therefore it is possible to term the total effect as secondary extinction, although the coherent domains are large enough to exhibit substantial dynamical effects.

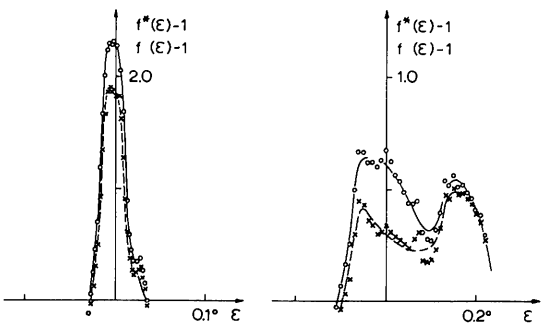

Fig. 3. The normalized ratio of the reflectivity for Mo $K\alpha$ radiation to that for Cu $K\alpha$ in the case of a narrow reflection (left), 10.0 at (−2,4), and a wide reflection (right), 10.1 at (−1,0). The values before a correction for secondary extinction, $f^*(\varepsilon) - 1$, are given by open circles (○), and those after the correction, $f(\varepsilon) - 1$, by crosses (×).

There are some considerable discrepancies among the structure factors included in Table 2, and the results must be scrutinized before interpreting these as physical quantities. Generally, small corrections, such as those to the wide reflections, cannot be much off from the correct value, if there is a fair correspondence between the reflection profiles measured with Mo $K\alpha$ and Cu $K\alpha$ radiations. On the other hand, corrections to the narrow reflections are large enough to make the validity of the Gaussian approximation (3) for $y_p[\delta(\varepsilon)]$ questionable. The model calculations (Olekhnovich & Olekhnovich, 1978, 1980) suggest that this approximation can be used when $y_p > 0{\cdot}5$. Correction to $r(\varepsilon)$ measured with Mo $K\alpha$ is 40% at most, but to the measurements with Cu $K\alpha$, which are needed as references, the corrections exceed the above limit with unpredictable consequences.

5. Measurements with polarized X-rays

The non-dispersive arrangement with very small beam divergence (0·1 mrad) is possible only when the beam transmitted through the Borrmann crystal is polarized perpendicular to the plane of diffraction. The other divergence is limited only by slits (see Fig. 1), and although the divergence distribution can be determined, it is usually too wide to make possible a deconvolution of the measured reflection profile. When the incident beam is polarized parallel to the plane of diffraction, $P_0 = P_{0,\parallel}$, only the integrated diffracted power can be determined;

$$\int P^*_{g,\parallel}(\varepsilon)\,\mathrm{d}\varepsilon = P_{0,\parallel} \exp(-\mu_0 T/\cos\theta) \int r^*_{\parallel}(\varepsilon)\,\mathrm{d}\varepsilon. \quad (8)$$

The reflectivity $\overline{\sigma_{\parallel}(\varepsilon)} = r_{\parallel}(\varepsilon)/(T/\cos\theta)$ can be solved only with an assumption of the shape of $r_{\parallel}(\varepsilon)$. Instead of doing this explicitly, we calculate directly the correction for primary extinction. From (4),

$$f(\varepsilon) = \sec^2 2\theta\{r_{\parallel}(\varepsilon)/r_{\perp}(\varepsilon)\}, \quad (9)$$

and with use of (5*b*)

$$y^{-1}_{p,\perp}(\varepsilon) = \{f(\varepsilon)\}^{1-\beta} = \{f(\varepsilon)\}^{\mathrm{cosec}^2 2\theta}. \quad (10)$$

The results from the measurements with two wavelengths suggest that $f(\varepsilon) - 1$, which is related to the correction for primary extinction through (4*b*), may be written in the following form,

$$f(\varepsilon) = 1 + \gamma\{r_{\perp}(\varepsilon)\}^p. \quad (11)$$

The measurement with parallel polarization is influenced by primary extinction less than that with perpendicular polarization, and it is seen from (9) that $f(\varepsilon) \geq 1$. Constant primary extinction corresponds to

Table 3. *Structure factors for* Be *from measurements with polarized* Cu $K\alpha$ *radiation*

The kinematical reflecting ratio $r_{kin}(\varepsilon)$ is calculated through the iterative procedure described in § 5. Parameter p refers to equation (11), and the most probable values are underlined; a broken line indicates a large uncertainty. The corresponding average extinction factors are given by $\overline{y}_{s,\perp}$ and $\overline{y}_{p,\perp}$.

hk.l	location	$p=0$	$p=0{\cdot}5$	$p=1$	$p=2$	$\overline{y}_{s,\perp}$	$\overline{y}_{p,\perp}$	F_{ave}
10.0	(0·5, −1)	1·892	1·897	1·903	1·911	0·915	0·785	1·90
	(−1, −2)	1·889	1·907	1·924	1·955	0·867	0·666	
	(−2, 4)	1·731	1·767	1·796	1·840	0·831	0·463	
00.2	(−1, 0)	3·395	3·403	3·409	3·420	0·831	0·871	3·37
	(−2, 4)	2·809	2·877	2·949	3·093	0·798	0·433	
10.1	(−1, 0)	2·756	2·761	2·766	2·775	0·852	0·850	2·78
	(−2, 4)	2·559	2·596	2·622	2·662	0·740	0·564	

$p = 0$, and if the corrections for both primary and secondary extinctions are proportional to $r_\perp(\varepsilon)$, $p = 1$. In the actual calculations the values $p = 0$, 0·5, 1, and 2 were used.

The parameter γ can be determined by an iterative procedure. With the use of (2) and (9), the observed integrated reflection is

$$\int r_\parallel^*(\varepsilon)\,d\varepsilon = \cos^2 2\theta \int \frac{r_\perp(\varepsilon) f(\varepsilon)}{1 + r_\perp(\varepsilon) f(\varepsilon) + \frac{1}{3}\{r_\perp(\varepsilon) f(\varepsilon)\}^2}\,d\varepsilon. \quad (12)$$

Upon substitution of the approximation (11) an algorithm is obtained,

$$\gamma_{n+1} = \frac{\sec^2 2\theta \int r_\parallel^*(\varepsilon)\,d\varepsilon - \int \{r_\perp(\varepsilon)/B\}\,d\varepsilon}{\int \{[r_\perp(\varepsilon)]^2/B\}\,d\varepsilon}, \quad (13a)$$

where

$$B = 1 + r_\perp(\varepsilon)\{1 + \gamma_n[r_\perp(\varepsilon)]^p\} + \tfrac{1}{3} r_\perp^2(\varepsilon)\{1 + \gamma_n[r_\perp(\varepsilon)]^p\}^2. \quad (13b)$$

The iteration converges rapidly, and a suitable starting value is

$$\gamma_1 = \{\sec^2 2\theta \int r_\parallel^*(\varepsilon)\,d\varepsilon - \int r_\perp^*(\varepsilon)\,d\varepsilon\} / \int \{r_\parallel^*(\varepsilon)\}^2\,d\varepsilon. \quad (13c)$$

A point-to-point correction of $r_\perp(\varepsilon)$ for primary extinction is calculated from (10) and (11).

Some of the results are given in Table 3, and examples of plots of the reflections at various stages of extinction corrections are shown in Fig. 4. Underlined values in Table 3 indicate the most probable values of p, as deduced from Fig. 3. The final structure factors, F_{ave}, are obtained by combining the data of varying wavelength and polarization, and the bounds in Table 4 are from the scatter of measurements where $\bar{y}_s$ and $\bar{y}_p$ were small. The values for the narrow reflections remain 5 to 10% smaller than F_{ave}, but even this is a remarkably good agreement, as the uncorrected integrated intensities may be only 35% of the final values, and the peaks $r_\perp(0)$ are on some occasions less than 20% of $r_{kin}(0)$. The corrected reflecting ratio, $r_{kin}(\varepsilon)$, exceeds unity for some reflections, which is an artefact arising from the calculation. The observed reflecting ratio is always less than 0·5, which would correspond to the balance of the direct and diffracted beam in an infinitely thick crystal.

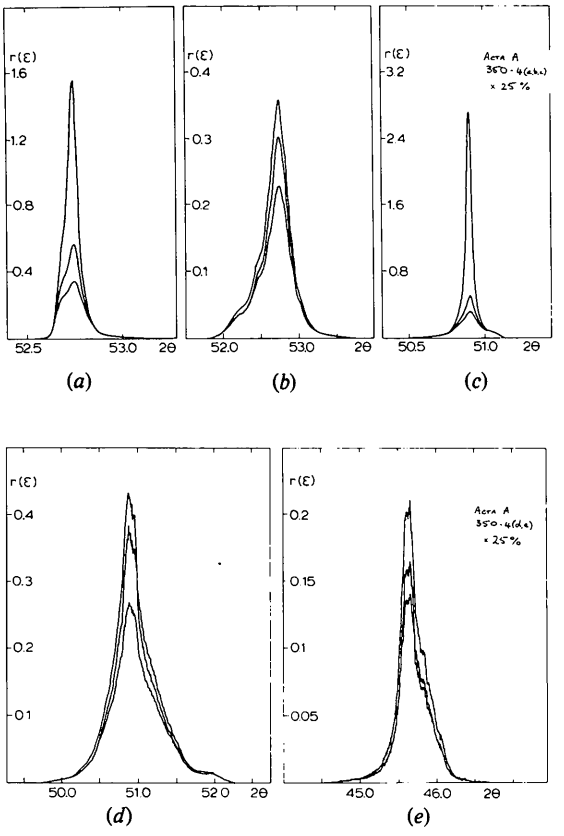

Fig. 4. Reflecting ratio in the measurements with polarized Cu $K\alpha$ radiation. The lowest curve is the measured reflection profile $r_\parallel^*(\varepsilon)$, the middle one, $r_\perp(\varepsilon)$, is corrected for secondary extinction, and the top curve is the kinematical profile calculated with equations (9) to (11). The scale is the same as in Fig. 2. (*a*) 10.1 at (−2,4), $p = 2$; (*b*) 10.1 at (−1,0), $p = 0$; (*c*) 00.2 at (−2,4), $p = 2$; (*d*) 00.2 at (−1,0), $p = 0$; (*e*) 10.0 at (0·5,−1), $p = 0$.

Table 4. *Experimental and theoretical structure factors of* Be *at room temperature*

These include a measurement from several crystal wafers with Ag $K\alpha$ radiation by Brown (1972) (B), γ-ray measurements and measurements from small crystals with conventional techniques using Ag $K\alpha$ radiation by Larsen, Hansen & Schneider (1981) (LHS), free-atom values from correlated wave functions (Benesch & Smith, 1970) (BS), a Wannier-function calculation (Matthai *et al.*, 1980 (MGM), and the results from a LCAO calculation (Dovesi *et al.*, 1981) (D). The theoretical values have been multiplied by the Debye–Waller factor $\exp(-B\sin^2\theta/\lambda^2)$, where $B_{11} = 0{\cdot}460$ Å^2 (in basal plane) and $B_{33} = 0{\cdot}415$ Å^2 (perpendicular to basal plane) (Manninen & Suortti, 1979).

hk.l	Present	B	LHS	BS	MGM	D
10.0	1·90 ± 0·01	1·715	1·86	1·774	1·824	1·914
00.2	3·37 ± 0·02	2·978	3·36	3·381	2·877	3·397
10.1	2·78 ± 0·03	2·606	2·82	2·879	2·696	2·810

6. Discussion

The present method of making corrections for extinction is purely experimental, it is based on operational definitions of primary and secondary extinctions, and it does not utilize any specified crystal model or theoretical structure factors. However, the crystal must be imperfect enough to make the method applicable. There must be a sufficient number of simultaneously diffracting incoherent domains to yield an average reflectivity $\overline{\sigma(\varepsilon)}$, which counts for the flow of intensity between the direct and diffracted beam. Primary extinction should be limited to $y_p \geq 0{\cdot}5$ to justify the Gaussian approximation, which is independent of the actual shape of the coherent domains.

The experimental conditions of the present study allowed only a partial utilization of the potential of the method, because the active volume and divergences could not be made identical in the measurements. However, when the correction for primary extinction is small, the actual shape of $y_p(\varepsilon)$ is not important, as seen in Table 3, and the average value can be deduced from the present data.

In the Be crystal studied the largest coherent domains were of the order of 10 μm in diameter, and accordingly each ray traversed about 100 domains. This is apparently sufficient for an ensemble average $\overline{\sigma(\varepsilon)}$. It was shown in I that large lateral fluctuations of $\sigma(\varepsilon)$ decrease the diffracted intensity from the value that would correspond to the volume average $\overline{\sigma(\varepsilon)}$. An indirect check of this possibility was made by using two different cross sections of the incident beam of Mo $K\alpha$ radiation, and the results were very consistent. The validity limit of the Gaussian approximation (4*a*) is exceeded in a few cases included in Tables 2 and 3, with variable consequences. On the other hand, good agreement between measurements where $\bar{y}_p$ remains small indicates that the Gaussian approximation for $y_p[\delta(\varepsilon)]$ seems to be able to accommodate the convolution by the distribution of the domain sizes.

The maximum reflecting ratio $r_\perp^*(0) = 0{\cdot}33$ was observed at the peak of the 00.2 reflection measured with Cu $K\alpha$ radiation at location (−2,4). This is close to the limiting value $r_\perp^*(\max) = 0{\cdot}5$, which is observed in thick perfect crystals, but the half-width of the reflection, $\Delta\varepsilon = 0{\cdot}07°$, is about 100 times larger than the Darwin width of 00.2. On the other hand, $\Delta\varepsilon$ is smaller by a factor of 5 than the half-width of the rocking curves of the best crystals of pyrolytic graphite. The peak reflecting ratio of Be 00.2 for Mo $K\alpha$ was observed to be 0·24. The effects of absorption are small for the crystal in question, as $\exp(-\mu_0 T/\cos\theta) = 0{\cdot}8$ for Cu $K\alpha$ and 0·95 for Mo $K\alpha$. High reflectivity and small absorption make Be a very suitable material for a medium-resolution transmission monochromator, provided that crystals of sufficient size can be grown (Hustache, 1979).

The structure factors of the first three reflections of Be are given in Table 4, which includes also previous experimental values and various theoretical results. The present values agree closely with the preliminary results by Larsen, Hansen & Schneider (1981), while the structure factors by Brown (1972) are low by 6 to 12%; this is presumably due to the combined effect of a too low scale and lack of extinction corrections (Manninen & Suortti, 1979; Larsen, Lehmann & Merisalo, 1980). The deviations from the free-atom values indicate strong static deformations of the atoms in solid. These are almost completely covered by a Hartree–Fock calculation by Dovesi, Pisano, Ricca & Roetti (1981), where an extended AO basis is used, and the same wave functions yield Compton profiles which agree closely with measurements (Dovesi, Pisano, Ricca & Roetti, 1982). The Wannier-function representation (Matthai, Grout & March, 1980) fails in the case of 00.2, but the other directions are rather well described.

The various recent studies of Be, which include elastic and inelastic neutron scattering (Larsen, Brown, Lehmann & Merisalo, 1982; Stedman, Amilius, Pauli & Sundin, 1976), X-ray diffraction, and Compton profile measurements (Loupias *et al.*, 1980, and references therein), give a coherent picture of the electron distributions of Be. This is concisely summarized by the LCAO calculation, but also other representations, such as Fourier maps of electron density or multipole expansions, may be illustrative. There are still minor discrepancies, which justify further studies, although these may rather serve to improve experimental techniques. This is very obvious in regard to the present method, which should be tested under ideal experimental conditions. A synchrotron radiation source provides a very parallel beam of linearly polarized X-rays with tuneable wavelength; all factors which are essential for an accurate determination of the extinction corrections with the present method.

It is my pleasure to extend belated thanks to J. J. DeMarco for collaboration and discussions during the preliminary studies on Be at Army Materials and Mechanics Research Center in 1970–71, and I am grateful to N. K. Hansen for communicating the latest results.

References

BENESCH, R. & SMITH, V. H. JR (1970). *Acta Cryst.* A**26**, 586–594.
BROWN, P. J. (1972). *Philos. Mag.* **26**, 1377–1394.
CHIPMAN, D. R. (1969). *Acta Cryst.* A**25**, 209–214.
COLE, H., CHAMBERS, F. W. & WOOD, C. G. (1961). *J. Appl. Phys.* **32**, 1942–1945.
DEMARCO, J. J., DIANA, M. & MAZZONE, G. (1967). *Philos. Mag.* **16**, 1303–1306.
DOVESI, R., PISANI, C., RICCA, F. & ROETTI, C. (1981). To be published.
DOVESI, R., PISANI, C., RICCA, F. & ROETTI, C. (1982). To be published.
HUSTACHE, R. (1979). *Nucl. Instrum. Methods*, **163**, 151–156.
INOUE, S. T. & YAMASHITA, J. (1973). *J. Phys. Soc. Jpn*, **35**, 677–683.
KURITTU, J. & MERISALO, M. (1977). Rep. Ser. Phys. No. 132. Univ. of Helsinki, Finland.
LARSEN, F. K., BROWN, P. J., LEHMANN, M. S. & MERISALO, M. (1982). *Philos. Mag.* B**45**, 31–50.
LARSEN, F. K., HANSEN, N. K. & SCHNEIDER, J. R. (1981). Unpublished.
LARSEN, F. K., LEHMANN, M. S. & MERISALO, M. (1980). *Acta Cryst.* A**36**, 159–163.
LOUPIAS, G., PETIAU, J., ISSOLAH, A. & SCHNEIDER, M. (1980). *Phys. Status Solidi B*, **102**, 79–95.
MANNINEN, S. & SUORTTI, P. (1979). *Philos. Mag.* B**40**, 199–207.
MATTHAI, C. C., GROUT, P. J. & MARCH, N. H. (1980). *J. Phys. F*, **10**, 1621–1626.
MERISALO, M. & KURITTU, J. (1978). *J. Appl. Cryst.* **11**, 179–183.
OLEKHNOVICH, N. M., MARKOVICH, V. L. & OLEKHNOVICH, A. I. (1980). *Acta Cryst.* A**36**, 989–996.
OLEKHNOVICH, N. M. & OLEKHNOVICH, A. I. (1978). *Acta Cryst.* A**34**, 321–326.
OLEKHNOVICH, N. M. & OLEKHNOVICH, A. I. (1980). *Acta Cryst.* A**36**, 22–27.
STEDMAN, R., AMILIUS, Z., PAULI, R. & SUNDIN, O. (1976). *J. Phys. F*, **6**, 157–166.
STEWART, R. F. (1977). *Acta Cryst.* A**33**, 33–38.
SUORTTI, P. (1982). *Acta Cryst.* A**38**, 642–647.
SUORTTI, P. & JENNINGS, L. D. (1977). *Acta Cryst.* A**33**, 1012–1027.
YANG, Y. W. & COPPENS, P. (1978). *Acta Cryst.* A**34**, 61–65.
ZACHARIASEN, W. H. (1967). *Acta Cryst.* **23**, 558–564.

Acta Cryst. (1982). A**38**, 656–663

Relaxation of Mackay Icosahedra

BY J. FARGES, M. F. DE FERAUDY, B. RAOULT AND G. TORCHET

Laboratoire de Physique des Solides, Université de Paris Sud, Bâtiment 510, 91405 *Orsay, France*

(*Received* 19 *January* 1981; *accepted* 29 *March* 1982)

Abstract

Multilayer icosahedra, first introduced about twenty years ago by Mackay [*Acta Cryst.* (1962), **15**, 916–918], are no longer considered a geometrical curiosity, as small icosahedral particles have been observed in a great number of experiments. The hard-sphere models, previously considered, are not really suited to the study of physical properties because they fail to express the important stresses due to the icosahedral structure. Therefore, Mackay icosahedra, made of atoms interacting through a Lennard-Jones potential, were constructed and allowed to relax freely. Results of the calculation are given, consisting of a detailed description of relaxed icosahedra with up to nine layers, *i.e.* with up to almost 3000 atoms.

0567-7394/82/050656-08$01.00

I. Introduction

Mackay (1962) noted that a cuboctahedron formed of rigid rods can be transformed into an icosahedron, it being sufficient for this that one of the diagonals of each square face be contracted to the length of the edge of a primitive cuboctahedron, while at the same time the face is folded following the same diagonal so as to form two equilateral faces (Fig. 1). This transformation to an icosahedron is very simple to visualize for a cuboctahedron of 13 atoms containing a single layer of atoms surrounding a central one, and for the cuboctahedron of 55 atoms, which contains an additional layer of atoms, it is sufficient that two layers are deformed at the same time, each square (100) face being transformed into two equilateral (111) faces. Thus to each cuboctahedron